THE JOURNAL OF PHYSICAL CHEMISTRY B

Article

Cite This: J. Phys. Chem. B 2019, 123, 3490−3498

pubs.acs.org/JPCB

Exploring the underlying mechanisms of the coupling between cell differentiation and cell cycle

Published as part of The Journal of Physical Chemistry virtual special issue "Deciphering Molecular Complexity in Dynamics and Kinetics from the Single Molecule to the Single Cell Level".

Kun Zhang[†] and Jin Wang*[,†,‡]

[†]State Key Laboratory of Electroanalytical Chemistry, Changchun Institute of Applied Chemistry, Chinese Academy of Sciences, Changchun, Jilin130022, P.R.China

[‡]Department of Chemistry and of Physics and Astronomy, Stony Brook University, Stony Brook, New York 11794-3400, United States

ABSTRACT: Differentiation and replication are the two major fates of the cells. They are the fundamental processes for completing the cellular functions. Although the underlying biological processes have been considerably explored for each of these processes and significant progresses have been made, global quantification and physical understanding are still challenging, especially for the relationship among them. In this study, we developed a theoretical framework for both the cell cycle and cell differentiation by exploring the associated global dynamics and their underlying relationship. We found that the dynamics of the cell cycle and cell differentiation is governed by both the landscape gradient and rotational curl flux. While landscape attracts the system down to the stable state basins, the curl flux drives the stable oscillation flow. We uncovered the irregular sombrero-shaped landscapes of the cell cycle at different developmental stages. We studied how the cells develop from undifferentiated cells to differentiated cells and how the cell cycle proceeds at different developmental stages. We investigated how the cell differentiation can influence the cell cycle where more progressive differentiation can lead to the changes of the cell cycle oscillations. In contrast, we can also quantitatively illustrate how the cell cycle can influence the cell differentiation where cell cycle regulation can lead to the changes of the differentiation processes. Through the landscape and flux analysis, we uncovered the key regulatory elements controlling the progression of the cell differentiation and cell cycle. This can help to design an effective strategy for drug discovery against associated diseases.

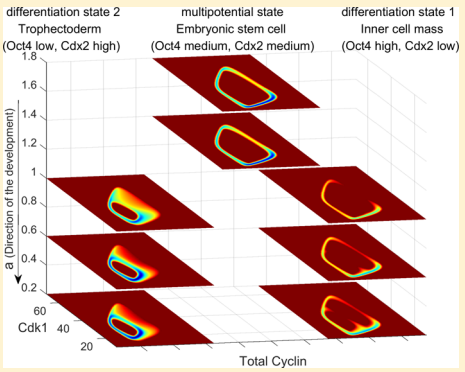

INTRODUCTION

The cells have two major fates. One is the differentiation and the other is the replication. The development of a multicellular organism involves many different organs and tissues and thus displays the integration of these two processes. One of the above-mentioned two processes is related to the phenotypic diversification of the cell populations by the completion of the cell fate decisions (cell differentiation). The other of the above-mentioned two processes is related to the increase of cellular amount or mass through the progress of the cell cycle. Both the cell fate decision and the cell cycle are crucial processes not only for the biological cell growth and proliferation but also for the maturation of the whole multicellular organism. Developmental cells change their phenotypes in an almost discontinuous manner, which manifest discrete developmental stages from multipotent stem cells to terminally differentiated types.

In the 1940s, Conrad Waddington proposed a qualitative picture of the epigenetic landscape to understand the dynamical pattern of the cell development. In this picture, a cell imagined as being a marble rolls down from the top of a hill and followed the pre-existing paths of the valleys of the surface (landscape). When it arrives in the watersheds, the "marble" makes a fateful decision and randomly chooses one of the two available paths. Once the developing cell chooses a possible path, it decreases the cellular potential and restricts its subsequent fate. Waddington's picture clearly hints the conceptions of stability and instability in the modern language of dynamics. Recently, Waddington's epigenetic landscape has been understood more quantitatively. This is due to the discovery of the genetic regulatory mechanisms for driving the cell development and the theoretical framework developed for providing the foundation and quantification of Waddington's landscape for the cell development and differentiation.

However, the biological cell duplicates its own components and divides into two daughter cells by the cell cycle to achieve the cell reproduction. The complete cell cycle is a periodic process that consists of four phases: the synthesis of DNA (S

Received: January 17, 2019
Revised: March 27, 2019
Published: April 1, 2019

DOI: 10.1021/acs.jpcb.9b00509
J. Phys. Chem. B 2019, 123, 3490−3498

phase), mitosis (M phase), and the two intervening phases G1 and G2. Sometimes, the cell also can stay in a quiescence state called the G0 phase where the cell temporarily stops dividing. A few checkpoints of the cell cycle dominate the sequence of the progression and thus enable the whole process to maintain the proper order. This mechanism can guarantee the beginning of the new phase dependent on the achievement of the pervious one.

With the profound understanding of the biology, it is now believed that both cell cycle and cell differentiation are delicately controlled by the underlying genetic regulatory mechanisms. Furthermore, the respective mathematical models have also been proposed to uncover the individual mechanisms of the cell cycle or differentiation. For example, the cell cycle is mainly controlled by the negative feedback loop composed of cyclin-dependent kinases (CDKs) and their associated cyclin protein, which dominate the process of the cell cycle.[1] The cell fate decision process is determined by a gene-circuit containing self-active and mutual repressive genes for controlling the cell differentiation. Meanwhile, the cell differentiation is tightly associated with the cell cycle in a biologic cell. The coupling between cell differentiation and the cell cycle has recently been investigated.[2−7] However, a quantitative framework of how the dynamics of a multigene regulatory circuit can coordinate the emergence of both cell cycle and cell differentiation has not been proposed yet.

Furthermore, the intrinsic fluctuations from the finite number of molecules and extrinsic fluctuations from the environments are present in the living cells.[8,9] Therefore, the stochastic feature should be considered in studying the cell cycle and the cell fate decisions in differentiation.[10−15] Although the stochastic nature of the gene regulatory network has been studied, it is still challenging to reach global quantifications and physical explanations for both the cell fate and the cell cycle together to uncover their joint underlying mechanisms.

In this work, we explore the global mechanisms of the cell cycle and the cell differentiation together on the basis of the gene regulatory network motif. We develop a theoretical framework to quantify the landscape for this regulatory gene circuit. The state space of the underlying gene regulatory network motif can represent the different gene expression patterns of the cell differentiation and the cell cycle. The occurrence of each gene expression pattern can be quantified by the probability distribution in the state space. Each state in the state space can occur with certain probability. The higher probability represents a larger chance of appearance and has higher chances of being observed in the experiments. The specific functional states or phases of the cell are closely related to the specific gene expression patterns, which often have higher probabilities (or lower potential valleys) on the landscape. By the quantifications of the underlying landscape and the associated probability flux, we can identify the driving force of the cell differentiation and the cell cycle and further explore the global stabilities of the undifferentiated or differentiated states and the flow of the cell cycle. We find that the driving force of dynamics is dependent not only on the gradient of potential landscape but also on the rotational curl flux. These two types of driving forces guarantee the cell fate stabilities of the normal development and differentiation, as well as the stability of the oscillation flows of the reproduction of the biological cell−cell cycle. Furthermore, we study how the cells develop from undifferentiated cells to differentiated cells and how the cell cycle proceeds at different developmental stages. Furthermore, we investigate how the cell differentiation can influence the cell cycle. We find the pluripotent transcript factor Oct4 can regulate the cell cycle by repressing phosphatases Cdc25. With the increase of related regulation, the period of the cell cycle oscillation in the cell differentiation state of higher level expression of Cdx2 is decreased significantly. We also explore how the cell cycle can influence the cell differentiation. We find cyclin-dependent kinases 1 can influence the cell fate by regulating transcript factor Cdx2. When the related regulation is increased to a threshold value, the multipotent stem cell only transforms to a certain differentiation state. We quantify the dissipation cost of the cell differentiation and the cell cycle while investigating dissipation consumption in different cellular phases. Through the landscape and flux analysis, we uncover the key regulatory elements controlling the progression of the cell differentiation and cell cycle. This can help to design an effective strategy for drug discovery against associated diseases.

MATERIALS AND METHODS

The mathematical model for the dynamics of the underlying gene regulatory network motif can be described by a set of ordinary differential equations with the driving force determined by the underlying gene regulations, synthesis and degradations. Through solving the ODEs, we can explore the dynamical behavior of the regulatory network. However, the intrinsic statistical fluctuations resulting from the finite number of molecules in the cell and external fluctuations from the cellular environments can influence the network dynamics. These indicate that the deterministic description cannot accurately capture the stochastic dynamics of the regulatory networks inside the cell. For the animal cells in our study, the number of molecules is often large within the cell. Thus, the intrinsic statistical fluctuations from the molecular numbers are expected to be small. Therefore, we only consider extrinsic fluctuations in this study. In this case, the mathematical model of the regulatory network motif dynamics can be expressed by the stochastic different equations with the noise term $\frac{dx}{dt} = F(x) + \eta$, where x is the concentration of the protein or gene expression levels and $F(x)$ is the dynamical driving force of the system. η is defined as Gaussian white noise with zero mean, and its autocorrelation function is defined as $\langle \eta(t)\, \eta(0) \rangle = 2D\delta(t)$, where D is the diffusion coefficient. This diffusion parameter characterizes the intensity of the intrinsic and cellular environmental fluctuations, with the diffusion coefficient being possibly concentration dependent.

Due to the presence of the stochastic fluctuations, even if the same initial conditions are given, the time evolution of the expression levels or concentration is not predictable. We can only obtain their statistical behavior by studying a large number of the trajectories. Therefore, a more appropriate quantitative representation can be utilized by the probability distribution evolution. By doing statistical analysis for the simulated trajectories, one can quantify the probability distribution function when the system reaches the steady state. However, the probability evolution follows the diffusion equations in the continuous case.[16] The diffusion equations are also called the Fokker−Planck equations, which have equivalent mathematical representation with the one by Langevin equations for describing the stochastic dynamics, one for the trajectory and another for the probabilistic

DOI: 10.1021/acs.jpcb.9b00509
J. Phys. Chem. B 2019, 123, 3490−3498

description. The Fokker−Planck equations can be formulated as a probability conservation law: $\partial P/\partial t + \nabla \cdot J = 0$, where J is the flux defined as the probability flux and dictated both by the deterministic driving force by the underlying chemical reactions of synthesis, degradation, activation, and repression regulations and by the stochastic force from the fluctuations characterized by the diffusion $J = FP - D\nabla P$. If the appropriate time-dependent solution $P(x,t)$ is obtained, it will describe not only the stationary behaviors but also the probability evolution dynamics of the systems.

In the steady state, $\partial P/\partial t = 0$, so that the divergence of flux $\nabla \cdot J = 0$ is zero. In the steady state, there are two possibilities here, one is the flux itself is zero. If that is the case, from the expression above we see that we can define a potential function U where $U = -\ln P_{ss}$ and P_{ss} represents the steady state probability. The driving force of the dynamics F can then be written as the gradient of the diffusion related to the inhomogeneity of the fluctuations $\nabla \cdot D$ and the gradient of the potential U, $-D \cdot \nabla U$. The flux $J = 0$ means no net input or output to or from the system. It is the detailed balance condition. So the system is in equilibrium. For an equilibrium system, the flux is zero and the whole system can be characterized by the potential U, which links directly to the probability by $U = -\ln P_{ss}$, the Boltzmann law. Here the P_{ss} represents the equilibrium probability. Furthermore, the dynamics is dictated by the gradient of the potential and the inhomogeneity of the fluctuations. Therefore, we uncovered the link between the equilibrium systems and the dynamical systems with detailed balance.[17]

However, for general dynamics of the general gene networks, the steady state does not necessarily satisfy the detailed balance condition, that is, $J_{ss} \neq 0$. In the general case, we can still define a potential landscape U as $U = -\ln P_{ss}$. The driving force now can be decomposed into three terms $F = -D \cdot \nabla U + J_{ss}/P_{ss} + \nabla \cdot D$,[17] the gradient of the potential U, $U = -\ln P_{ss}$; the steady state flux-dependent term J_{ss}/P_{ss}; and diffusion-coefficient-dependent term $\nabla \cdot D$. (The last term is the derivative of the fluctuation strengths or the diffusion coefficient with respect to the concentrations. For the animal cells, the intrinsic statistical fluctuations due to the molecular numbers are usually small. Therefore, only the extrinsic fluctuations are considered in this study, which is assumed to be independent of the expression levels or concentrations. In this case, the derivative term is usually zero.) Since the flux is not zero, there is a net input or output to or from the environment. The detailed balance condition is not satisfied. The system is at nonequilibrium. In fact, the flux quantitatively measures the degree of detailed balance breaking. Since the flux satisfies the divergent free property in the steady state, the contribution to the driving force has a curl nature. This is because there can be no sources or sinks for the divergent free flux lines to go into and come out. The only way for the nonzero flux is to rotate around.

Therefore, we can establish a link between the general network dynamics and the nonequilibriumness of the system. The global nature of the network can still be described by a potential landscape U since the U is directly related to the steady state probability, which quantifies the weights of each state of the whole network for global characterization. The dynamics, however, is not only determined by the gradient of the potential and inhomogeneity of the fluctuations as in the equilibrium systems. There exists an additional contribution to the driving force coming from the nonzero flux that breaks the detailed balance. A global description is still in terms of the potential landscape reflecting the steady state probability. However, distinctly different from equilibrium dynamics, the driving force is determined not only by the gradient of the potential but also by the curl flux. Therefore, equilibrium dynamics is analogous to an electron moving in an electric field while the nonequilibrium system dynamics is analogous to an electron moving in an electric and a magnetic field.

For the two-dimensional or three-dimensional systems, we can work out the landscape by directly solving the Fokker−Planck equation and obtain the steady state distribution for quantifying the landscape and flux. In this multidimensional system, it is difficult to solve directly the Fokker−Planck equation numerically due to the memory issues for the partial differential equation. Here, we collect the statistics of the simulated trajectories to obtain the probability distribution at steady state. More concretely, the probability distribution can be quantified and obtained from the long time simulated trajectories of the underlying stochastic Langevin dynamics for the gene expressions/protein concentrations. To visualize the landscape, we reduce the four-variable probability distribution to a three-variable distribution by introducing a new variable X_c to represent the two of the four variables.

The biological system can exchange the energy, materials, and information with the environments. This can generate dissipation. The system entropy can be defined as $S = -\int P(x,t) \ln P(x,t)\, dx$. By differentiation of the above the formula, the change rate of the system entropy can be written as $\dot{S} = \int (J \cdot D^{-1} \cdot J)/P\, dx - \int (J \cdot D^{-1} \cdot (F - \nabla \cdot D))\, dx$, where $\int (J \cdot D^{-1} \cdot J)/P\, dx = e_p = \dot{S}_{tot}$ is defined as the entropy production rate(EPR). It denotes the total entropy change rate (including both system and environment). $\int (J \cdot D^{-1} \cdot (F - \nabla \cdot D))\, dx = h_d = \dot{S}_{env}$ is the rate of the heat dissipation or the entropy change rate from the environment. When the nonequilibrium system is in a steady state, the change rate of the system entropy $\dot{S}$ is equal to zero. Therefore, the heat dissipation from the environment in the steady state is equal to the total entropy production rate of the nonequilibrium system and the environment.[18,19] According to this equation, the energy dissipation h_d can be quantified by the total entropy production e_p, which is related directly to the curl flux J. The more nonequilibrium is, the larger the flux is and the more the dissipation is. The entropy rate equation can also be written as $\dot{S}_{tot} = \dot{S} + \dot{S}_{env}$. This gives the first law of nonequilibrium thermodynamics. The entropy production is always larger or equal to zero. This gives the second law of nonequilibrium thermodynamics.[18]

RESULTS AND DISCUSSION

Gene Regulatory Network Motif of Differentiation and Cell Cycle. A gene regulatory circuit motif or wiring diagram determining the developmental cell fates and cell cycle is shown in Figure 1. In this simplified motif, the network consists of two mutual regulated modules. On top of the wiring diagram, the cell cycle module mainly controls the process of the mitosis. The mitotic cyclin synthesis is represented by a constant rate k_s. The newly synthesized cyclin is converted to cyclin−Cdk1 complexes and rapidly phosphorylated by the Cdk-activating kinase CAK. Under this condition, the mitotic cyclin generates active Cdk1−cyclin. These complexes can be inactivated by kinases Wee1A and reactivated by phosphatase Cdc25. Both active and inactivated Cdk1−cyclin complexes can also be eliminated through cyclin degradation with the increase of activation of ubiquitin ligase APC/C^{Cdc20} by active

DOI: 10.1021/acs.jpcb.9b00509
J. Phys. Chem. B 2019, 123, 3490−3498

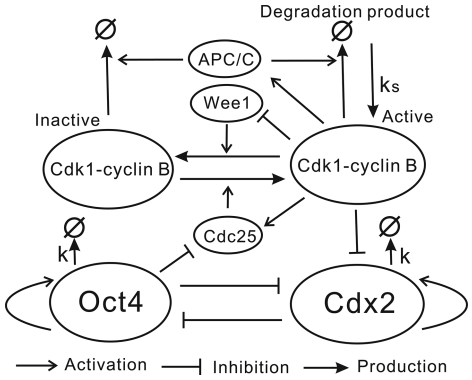

Figure 1. Wiring diagram for cell cycle and cell differentiation gene regulatory circuit motif.

Cdk1.[20] The periodic changes of the mitotic cyclin and the active Cdk1−cyclin represent the progression of the cell cycle. At the bottom of the wiring diagram, the self-activation and mutual inhibition regulations between transcription factor Oct4 (octamer-binding transcription factor 4) and Cdx2 govern the binary cell fate decision making process of differentiation. Oct4 is known as pluripotent transcription factor playing an essential role in maintaining the pluripotency state of self-renewing stem cells. The high expression of Oct4 induces stem cell differentiation into inner cell mass. However, the high expression of Cdx2 leads to the formation of trophectoderm differentiated state from the pluripotent stem like state. Meanwhile, the genes of the two modules of the cell differentiation and cell cycle can also mutually regulate each other. Oct4 can repress the reactivation of Cdk1 complexes by inhibiting phosphatases Cdc25 and influence on the progression of the cell cycle. The Cdk1 complexes can repress the expression of transcription factor Cdx2 and influence the cell differentiation.[21,22] These genes and regulations collectively determine how the multipotent progenitor cell divides into two daughter cells and differentiates into adult cell.

Mathematical models of the cell differentiation or the cell cycle have been proposed, respectively.[20,23−34] The understanding of the cell cycle, proliferation, and differentiation together is still challenging due to the less clear knowledge on the mutual regulation of cell differentiation and the cell cycle. In this study, we associate the simplest regulatory motif of the cell cycle with the simplest cell fate module to explore the cell division, proliferation and differentiate process. In the kinetic scheme, the hollow arrow represents the activation or self-activation between two proteins. It can be quantitatively formulated by the Hill function in the model equation. For example, activating Cdk1−cyclin complex activates the APC/C^{Cdc20}. The ⊥ represents the repression between two proteins. It can be quantitatively formulated by the Hill function of repression. For example, Oct4 represses Cdx2. The cross sign between the hollow arrow and solid arrow represents the production or degradation. It can be quantitatively formulated by kB. B represents the reactant concentration, and k denotes activation rate. For example, total mitotic Cdk1−cyclin (active cdk1−cyclin and inactive cdk1−cyclin) degrades. On the basis of the above gene regulatory wiring diagram, we build the model represented by the following four equations

$$\frac{\mathrm{d}}{\mathrm{d}t}\mathrm{Cyc} = k_s - ka_{\mathrm{deg}}\cdot Cyc$$

$$\frac{\mathrm{d}}{\mathrm{d}t}\mathrm{Cdk1} = k_s + ka_{\mathrm{cdc}}(\mathrm{Cyc} - \mathrm{Cdk1}) - kr_{\mathrm{wee1}}\cdot\mathrm{Cdk1} - ka_{\mathrm{deg}}\cdot\mathrm{Cdk1}$$

$$\frac{\mathrm{d}}{\mathrm{d}t}\mathrm{Oct4} = ka_{\mathrm{Oct4}} + kr_{\mathrm{Cdx2}} - k\cdot\mathrm{Oct4}$$

$$\frac{\mathrm{d}}{\mathrm{d}t}\mathrm{Cdx2} = ka_{\mathrm{Cdx2}} + kr_{\mathrm{Oct4}} + kr_{\mathrm{Cdk1}} - k\cdot\mathrm{Cdx2}$$

Here, the first equation describes the synthesis and degradation of the total mitotic cyclins. In our model, this concentration is equal to the sum of the inactive and active Cdk1−cyclin complexes. k_s represents the rate constant of cyclin synthesis. ka_{deg} represents the rate constant of cyclin degradation varied with the activity of Cdk1 as a result of the activation of APC/C^{Cdc20} by Cdk1 and can be described by the Hill function: $ka_{\mathrm{deg}} = a_{\mathrm{deg}} + b_{\mathrm{deg}}\frac{\mathrm{Cdk1}^{n_{\mathrm{deg}}}}{S_{\mathrm{deg}}^{n_{\mathrm{deg}}} + \mathrm{Cdk1}^{n_{\mathrm{deg}}}}$. The second equation describes the production of active Cdk1−cyclin complexes. The parameter ka_{cdc} represents the production rate of protein Cdc25C, which can reactivate Cdk1 by removing phosphate. The rate kr_{wee1} denotes the production rate of protein kinase Wee1A, which can accelerate the conversion from the active Cdk1 to inactive Cdk1 complexes. ka_{cdc} is a function of the active Cdk1 concentration and the expression level of Oct4. kr_{Wee1} is a function of the active Cdk1 concentration. Their steady state response was determined by the experimental studies and can be approximated by the Hill functions:[20,35,36] $ka_{\mathrm{cdc}} = a_{\mathrm{cdc}} + b_{\mathrm{cdc}}\frac{\mathrm{Cdk1}^{n_{\mathrm{cdc}}}}{S_{\mathrm{cdc}}^{n_{\mathrm{cdc}}} + \mathrm{Cdk1}^{n_{\mathrm{cdc}}}} + b_{23}\frac{S^n}{S^n + \mathrm{Oct4}^n}$, $kr_{\mathrm{wee1}} = a_{\mathrm{wee1}} + b_{\mathrm{wee1}}\frac{S_{\mathrm{wee1}}^{n_{\mathrm{wee1}}}}{S_{\mathrm{wee1}}^{n_{\mathrm{wee1}}} + \mathrm{Cdk1}^{n_{\mathrm{wee1}}}}$. The third equation and the final equation describe the production and degradation of Oct4 and Cdx2. Their regulations were determined by the experimental studies and can also be represented by the Hill equation:[31,32,37] $ka_{\mathrm{Oct4}} = a\frac{\mathrm{Oct4}^n}{S^n + \mathrm{Oct4}^n}$, $kr_{\mathrm{Cdx2}} = b\frac{S^n}{S^n + \mathrm{Cdx2}^n}$, $ka_{\mathrm{Cdx2}} = a\frac{\mathrm{Cdx2}^n}{S^n + \mathrm{Cdx2}^n}$, and $kr_{\mathrm{Cdk1}} = b_{42}\frac{S_{42}^n}{S_{42}^n + \mathrm{Cdk1}^n}$

Table 1. Parameters for the Four-ODE Computational Model

parameter	value	parameter	value	parameter	value
a_{deg}	0.01 min^{-1}	a_{cdc}	0.16 min^{-1}	a_{wee1}	0.08 min^{-1}
b_{deg}	0.04 min^{-1}	b_{cdc}	0.8 min^{-1}	b_{wee1}	0.4 min^{-1}
n_{deg}	17	n_{cdc}	11	n_{wee1}	3.5
S_{deg}	32 nM	S_{cdc}	35 nM	S_{wee1}	30 nM
a	1 min^{-1}	b	1 min^{-1}	n	4
S	0.5 nM	k	1 nM/min		
k_s	1 nM/min	S_{42}	30 nM		
b_{23}	0.1 min^{-1}	b_{42}	0.1 min^{-1}		

DOI: 10.1021/acs.jpcb.9b00509
J. Phys. Chem. B 2019, 123, 3490−3498

As shown is Table 1, we display the related rate parameters for the gene regulatory circuit motif model. The regulation parameters for the developmental and cell cycle modules are chosen from the related experimental studies or the classical model studies.[20,31,35−39] In our work, the developmental module and cell cycle module can mutually regulate each other through two regulations quantified by the regulation strength parameters b_{23} and b_{42}. Therefore, we mainly focus on these two regulation parameters for the coupling of the two modules while keeping other parameters fixed to explore how the cell cycle and cell differentiation influence each other. Meanwhile, we assume the rate of the parameter change is much slower than the relaxation time scale. This is reasonable because the parameter change is often coming from the environment. The environmental changes are often much slower than the gene regulation dynamics. Therefore, in this case, the probability evolution can reach the steady state for a specific fixed set of parameters(mimicking a fixed environment).

Note that the regulations between the cell cycle module and the cell differentiation module are from the repression of Oct4 to the active Cdk1 through repressing the Cdc25 (differentiation to cell cycle) and from the repression of Cdk1 to Cdx2 (cell cycle to differentiation).

Landscape and Flux of the Cell Cycle and Cell Differentiation. On the basis of the above mathematical model of the cell cycle and cell differentiation, we explore the associated stochastic dynamics. By following the probabilistic evolution, we can obtain the steady state probability distribution in the state space. The quantitative landscape of the cell cycle and differentiation with the fixed parameters are shown in Figure 2. In the visual landscape representation, the different colors represent the different depths of the potential landscape U (inversely related to the probability landscape P_{ss}: $U = -\ln P_{ss}$). The red denotes the higher landscape potential U while the blue denotes the lower landscape potential U. Total cyclin axis and Cdk1 axis denote the expression levels of the total mitotic cyclin and active Cdk1, respectively. The X_c axis denotes the distance between the current cell state and the diagonal line of Oct4 and Cdx2 expression plane. Because the expression level of the two opposing fate determining transcription factors is equal at the diagonal line of Oct4 and Cdx2 expression plane, this type of cells often stays in the undifferentiated undecided multipotent stem cell state. Therefore, the plane of $X_c = 0$ represents the undifferentiated cell state, and the plane of $X_c > 0$ and $X_c < 0$ represents the two types of differentiated cell state with mutually excluding expression of Oct4 and Cdx2. We see that the landscape has an irregular sombrero shape in different cell states. For the 3-dimensional landscapes in different cell states, the red center region (hat region of the sombrero shape) is higher in potential while the blue region (the ring valley region of the sombrero shape) has the potential lower than that of the red center. The outside of the ring region also (edge region of the sombrero shape) has higher potential. The topography of the landscape is an inhomogeneous irregular sombrero shape. The different sombrero shape has different color contrast on the landscape. The deeper color contrast indicates that the cell cycle proceeds more easily in the cell differentiation stages. The shape of the sombrero topography of the landscape implies that when starting anywhere in the state space, the gradient of the landscape will drive the state to the ring region of the landscape since the potentials there are relatively lower than the other regions of the state space. This guarantees the stabilities of the states on the ring. This is analogous to the situation of the river in the mountain where the river has the lowest height so that everywhere else on the mountain the water flows down to the nearest place in the river. However, once the states are stabilized on the ring valley, the states tend to stay in the lowest potential region on the ring valley. This does not support a stable oscillation flow. For a stable oscillation, there is a need for a rotational force driving the dynamics along the close ring valley. This is provided by the steady state probability flux. Therefore, the steady state probability flux with the curl rotational nature guarantees the stability of the oscillation flow while the landscape guarantees the stabilities of the states on the oscillation ring valley. While the landscape gradient attracts the system down to the oscillation ring valley, stabilizing the states on the oscillation path, the flux drives the stability of the cell cycle flow.

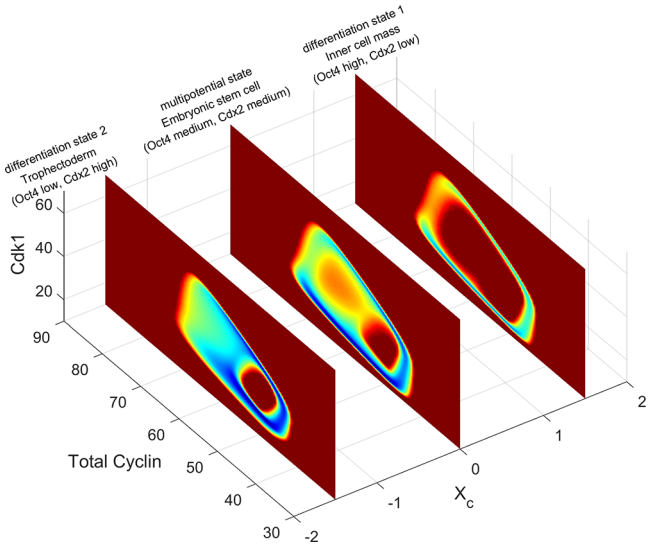

Figure 2. Landscapes of cell cycles at multipotent and differentiated states. X_c = Oct4 $\cos(\pi/4)$ − Cdx2 $\sin(\pi/4)$ represents the distance between the current cell state and undifferentiated cell state. Total cyclin concentration is equal to the sum of concentrations of active and inactive Cdk1−cyclin complexes. Cdk1 represents the concentration of active Cdk1−cyclin complexes.

During the cell developmental process, the changes of the self-activation strength of the transcription factors Oct4 and Cdx2 provide a significant measure and the direction of the development. When the self-activation is strong (characterized by large value of self-activation parameter a), the cell is more preferred to stay in the undifferentiated multipotent stem cell state. When the self-activation is weaker, the cell is preferred to be at differentiated states. With the continual decrease of self-activation, finally the stem cell becomes unstable and only stays in the differentiated states. The gradually decrease of self-activation parameter a manifests one possible mechanism for the development from undifferentiated stem cell to one of the two types of differentiated cells. Through the change of the self-activation parameter a, we can quantitatively map out the landscape of cell cycle at different developmental stages, as shown in Figure 3. The vertical axis represents the different developmental stage by the change of self-activation strength parameter a. For the different self-activation parameters, Figure 3 shows the different planes representing the different cell

DOI: 10.1021/acs.jpcb.9b00509
J. Phys. Chem. B 2019, 123, 3490−3498

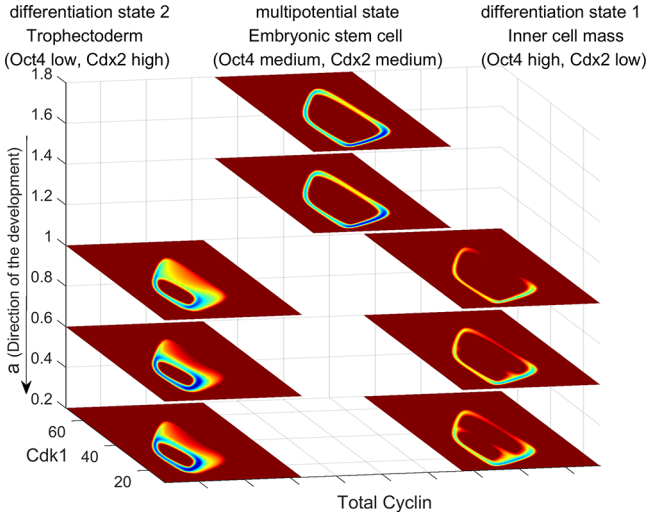

Figure 3. Landscapes of cell cycles at different developmental stages. Regulation parameter *a* represents the self-activation and the direction of the development. The landscapes of the cell cycles gradually change in different developmental stages.

differentiation stages. The right and left planes display the two types of the differentiated cell states at different stages of differentiation. The left plane represents the differentiation state 2 for the high level expression of Cdx2 in the cell. The right plane represents the differentiation state 1 for the high level expression of Oct4. The center plane denotes the undifferentiated multipotential stem cell state. When the self-activation is strong, we can see the emergence of the cell cycle at the center of the three planes. The multipotent stem cell state can enter into the mitosis of cell cycle. With the decrease of the self-activation strengths parameter *a*, the oscillation ring with the sombrero shape in the middle of the planes gradually disappears. The probability or the chance of the cell cycle emergence reduces for the multipotent stem cell state. Meanwhile, a clear cell cycle ring with the sombrero shape appears on the left plane representing robust oscillation of cell cycle as differentiation progresses. We can see the cell makes a fate decision and enters into one of the differentiated states.

Influence on Cell Cycle from Cell Differentiation. To investigate the dynamics and the thermodynamic dissipation consumption of the cell cycle at different cell stages, we calculate the integral of flux along the limit cycle, the entropy production rate(EPR), and period of cell cycle oscillation at different cell differentiation stages with different regulation parameters.

As shown in Figure 4a,b, the flux and EPR increase with the increase of the regulation parameter b_{23} in the differentiation state 2. But the change of the EPR and flux is small with the increase of parameter b_{23} in the differentiation state 1 and multipotent state. The regulation parameter b_{23} denotes the maximum generation rate from the regulation of Octamer-binding transcription factor 4 (Oct4) to the kinase Cdk1 by repressing Cdc25. In Figure 4c, we plot the change of period of cell cycle oscillation with the regulation parameter b_{23}. We can see the period decreases with the increase of b_{23} in the differentiation state 2. The change of period of cell cycle oscillation is small in the differentiation state 1 and multipotent state. This shows that the flux and associated thermodynamic dissipation (EPR) can significantly influence period of cell cycle oscillation. The increase of regulation parameter b_{23} can accelerate the cell cycle on the differentiation state 2 by stronger flux and more associated dissipation of energy per unit time. Furthermore, we can also see that the period of cell cycle oscillation in the differentiation state 1 is longer than in the other states in all the range of the regulation parameter b_{23}. Due to high expression level of Oct4 in the differentiation state 1, the longer period shows the inhibition function from Oct4 to the cell cycle. Our results are consistent with the correlated experimental study, which reported ectopic expression of Oct4 can delay the mitotic entry and elongate the progression of cell cycle.[21]

In Figure 5a–c, we plot the relationship between the entropy production rate and the flux in three cell states. The entropy production quantifies the input energy supply or consumption. We show that the entropy production rate is positively related to the integral flux along the limit cycle in all of the cell states. This indicates that the consumption of energy of the system is tightly correlated with the flux of the cell cycle. Since the rotational curl flux is the driving force for the cell cycle flow and dynamical requirement for the emergence of a

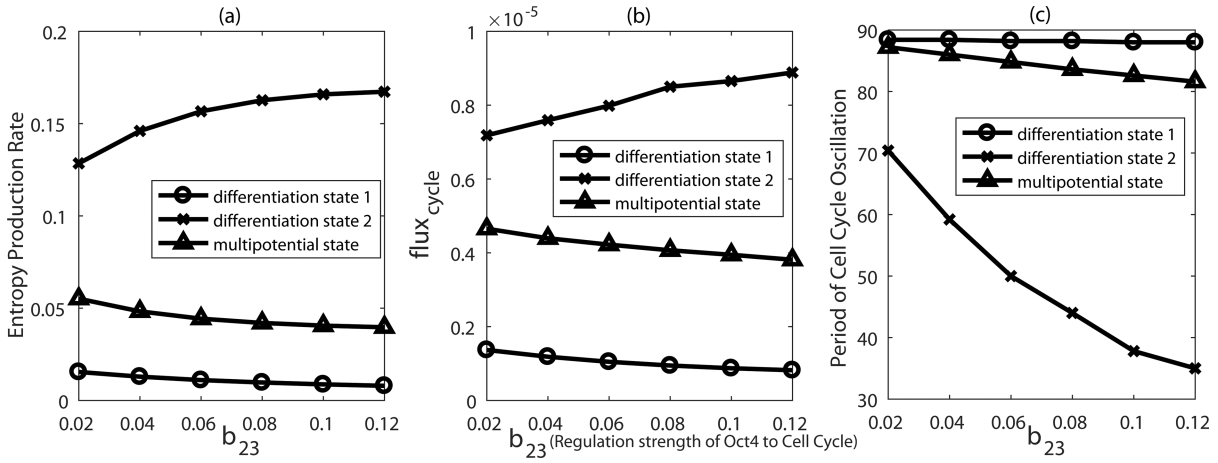

Figure 4. (a) Entropy production rate of the different cell states at different regulation parameters b_{23}. Regulation parameter b_{23} represents the regulation strength of Oct4 to cell cycle by repressing the phosphatase Cdc25. (b) Integral of flux along the limit cycle of the different cell states at different regulation parameters b_{23}. (c) Period of the cell cycle oscillation of the different cell states at different regulation parameters b_{23}.

DOI: 10.1021/acs.jpcb.9b00509
J. Phys. Chem. B 2019, 123, 3490−3498

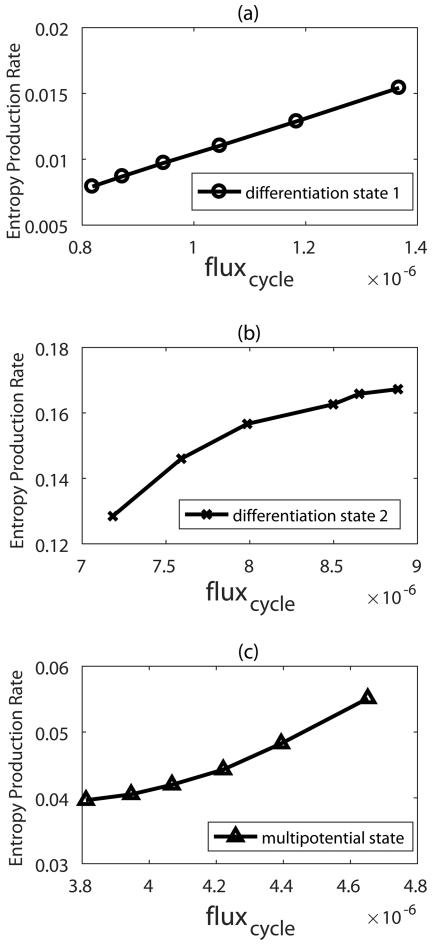

Figure 5. Entropy production rate versus the integral of flux along the limit cycle $\oint J\,\mathrm{d}l/\oint \mathrm{d}l$ in three cell states: (a) differentiation state 1; (b) differentiation state 2; (c) multipotential state.

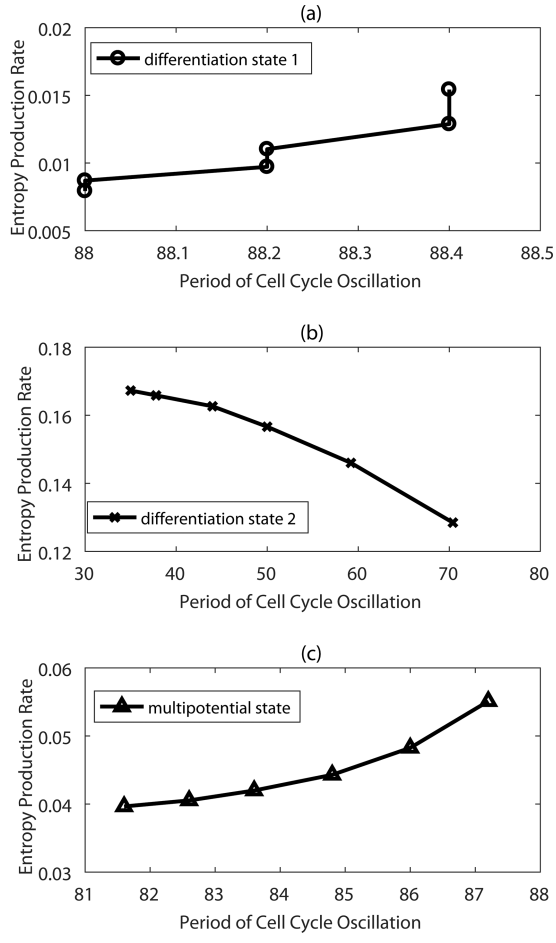

Figure 6. Entropy production rate versus period of cell cycle oscillation in three cell states: (a) differentiation state 1;(b) differentiation state 2; (c) multipotential state.

new stable phase (cell cycle), the production and progression of the cell cycle originates from the input of energy or nutrition supply.

In Figure 6a–c, we show the relationship between period of cell cycle oscillation and entropy production rate in the different regulation parameter b_{23}. We can see EPR increases with an increase of the cell cycle oscillation period in the multipotential state and differentiation state 1. But the EPR decreases with an increase of the period of cell cycle oscillation in differentiation state 2. In the multipotent state and differentiation state 1, the inhibition effect for the cell cycle strengthens because of higher expression of Oct4. This slow down in period of cell cycle oscillation comes from the more tight repression regulation, which requires more input energy supply through entropy production to support. In the differentiation state 2, high expression of Cdx2 does not repress the cell cycle. Thus the higher entropy production rate can accelerate the progression of cell cycle.

Influence on Cell Differentiation from Cell Cycle. Through the change of the regulated parameter b_{42}, we can quantitatively map out the landscape of the cell cycle at different regulation parameters b_{42}, as shown in Figure 7. The regulation parameter b_{42} denotes the regulation strength of Cdk1 to transcript factor Cdx2. It represents a regulation connecting cell cycle to cell differentiation. As shown in Figure 7, the stem cell state and two differentiation states have the

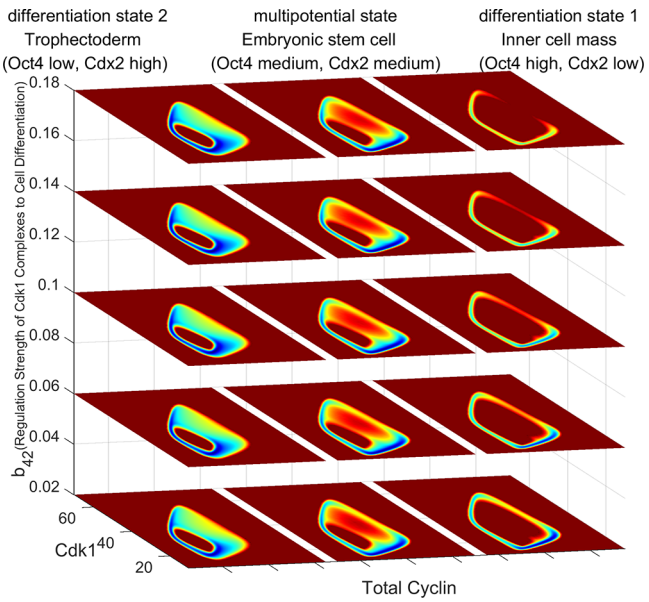

Figure 7. Landscape of cell cycle and cell differentiation at different regulation parameters b_{42}. Regulation parameter b_{42} represents the regulation strength of Cdk1 complexes to cell differentiation.

complete ring shape landscape of the cell cycle at the lower values of regulation parameter b_{42}. With the increase of

DOI: 10.1021/acs.jpcb.9b00509
J. Phys. Chem. B 2019, 123, 3490−3498

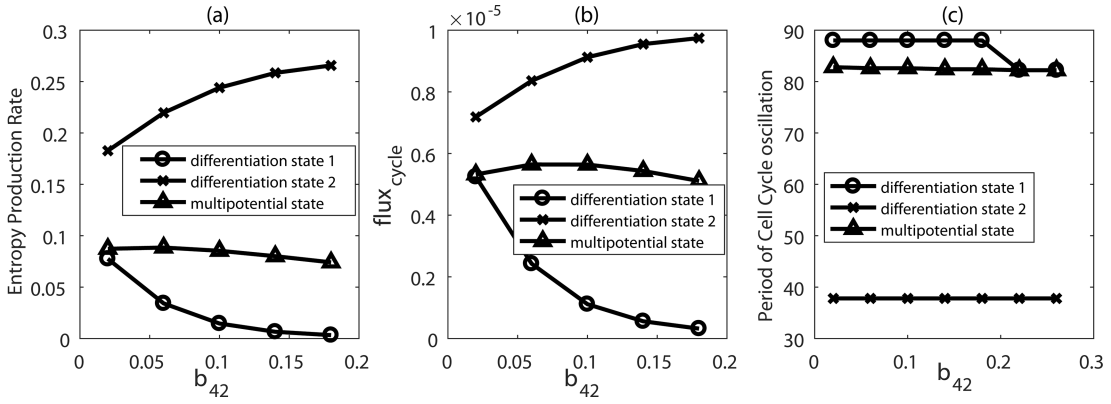

Figure 8. (a) Entropy production rate of the different cell states at different parameters b_{42}. With the increase of regulatory parameter b_{42}, the regulation strength of Cdk1 to cell differentiation is changed. (b) Integral of flux along the limit cycle of the different cell states at different regulation parameters b_{42}. (c) Period of cell cycle oscillation of the different cell states at different regulation parameters b_{42}.

regulation parameter b_{42}, the landscape in the differentiated state 1 eventually cannot shape a closed loop. This shows that the cell differentiation can only enter into certain differentiation state 2 (trophectoderm) when the regulation b_{42} increases beyond a certain threshold value. In this differentiation state, the expression level of transcript factor Cdx2 becomes high and the expression level of Oct4 becomes lower. Therefore, we can see that the cyclin-dependent kinases 1 (Cdk1) mainly controlling the cell cycle can also regulate the differentiation of the stem cells.

As shown in Figure 8a,b, we plot the integral of flux along the limit cycle and EPR at different repression regulation parameters b_{42}. When the regulation b_{42} is small, the flux or EPR results of the different cell states are almost equal. Under this condition, the cell fate is not influenced by the regulated gene Cdk1 from the cell cycle. With the increase of the regulation parameter b_{42}, the flux and dissipation cost EPR of the differentiation state 2 increase. Meanwhile, the flux and dissipation cost EPR of the differentiation state 1 gradually decrease. When the EPR reaches a threshold value, not enough energy can support the completion of the cell cycle progression in the differentiation state 1. The differentiation state 1 disappears from the possible cell states. The multipotential stem cell can only be differentiated and enter into the differentiation state 2. In Figure 8c, we can see the period of the multipotential state is equal to that of the differentiation state 1. Therefore, the differentiation state 1 and multipotential state merge when the regulation parameter b_{42} is more than 0.2. By the changes of the oscillation periods in different cell states, we can further see that Cdk1 can also regulate the differentiation of the stem cells.

CONCLUSIONS

In this work, we developed a theoretical framework to uncover the underlying mechanism of the interplay between the cell differentiation and cell cycle. On the basis of the gene regulatory network motif, we show the cell cycle at the developmental stages evolves from the undifferentiated state to the differentiated state. We quantitatively uncovered the driving forces for the dynamics of the cell cycle and cell differentiation as the negative gradient of landscape and the curl flux. The landscapes at different states of the differentiation and development show irregular sombrero shapes. While the gradient force of the landscape guarantees the stability of the states on the cell cycle path, the curl flux drives the stable oscillation flow of the cell cycle. Through our theoretical framework, we explained quantitatively how the cell differentiation influences the cell cycle. In contrast, we also explained quantitatively how the cell cycle influences the cell differentiation. We studied the regulations between the cell cycle and cell differentiation through the change in the regulation parameters. We found that the pluripotent transcript factor Oct4 can influence the progression of the cell cycle by the regulation of Cdk1 reactivation. With the increase of the related regulation, the period of cell cycle oscillation in the cell differentiation state of a high level expression of Cdx2 is decreased significantly. Meanwhile, we found cyclin-dependent kinases 1 can influence the cell differentiation by regulating the transcript factor Cdx2. With the increase of related regulation, the multipotent stem cell can transform into a certain differentiation state. Through the landscape and flux analysis, we uncovered the key regulatory elements (b_{23} and b_{42}) by controlling the progression of the cell differentiation and cell cycle. This can help to design an effective strategy for drug discovery against associated diseases.

AUTHOR INFORMATION

Corresponding Author

*E-mail: jin.wang.1@stonybrook.edu.

ORCID

Jin Wang: 0000-0002-2841-4913

Notes

The authors declare no competing financial interest.

ACKNOWLEDGMENTS

J.W. thanks Prof. Marc Kirschner and Prof. James Ferrell for helpful discussions. We thank the support of National Nature Science Foundation of China Grants No. 21721003 and Most, China, Grant No.2016YFA0203200. J.W. thanks support in part by NSF-PHY-76066 and NSF-CHE-1808474.

REFERENCES

(1) Nurse, P.; Masui, Y.; Hartwell, L. Understanding the cell cycle. *Nat. Med.* **1998**, *4*, 1103−1106.

(2) Dalton, S. Linking the Cell Cycle to Cell Fate Decisions. *Trends Cell Biol.* **2015**, *25*, 592−600.

(3) Li, V. C.; Kirschner, M. W. Molecular ties between the cell cycle and differentiation in embryonic stem cells. *Proc. Natl. Acad. Sci. U. S. A.* **2014**, *111*, 9503−9508.

DOI: 10.1021/acs.jpcb.9b00509
J. Phys. Chem. B 2019, 123, 3490−3498

(4) Pauklin, S.; Vallier, L. The Cell-Cycle State of Stem Cells Determines Cell Fate Propensity. *Cell* **2013**, *155*, 135−147.
(5) Ruijtenberg, S.; van den Heuvel, S. Coordinating cell proliferation and differentiation: Antagonism between cell cycle regulators and cell type-specific gene expression. *Cell Cycle* **2016**, *15*, 196−212.
(6) Soufi, A.; Dalton, S. Cycling through developmental decisions: how cell cycle dynamics control pluripotency, differentiation and reprogramming. *Development* **2016**, *143*, 4301−4311.
(7) Budirahardja, Y.; Gonczy, P. Coupling the cell cycle to development. *Development* **2009**, *136*, 2861−2872.
(8) Swain, P. S.; Elowitz, M. B.; Siggia, E. D. Intrinsic and extrinsic contributions to stochasticity in gene expression. *Proc. Natl. Acad. Sci. U. S. A.* **2002**, *99*, 12795−12800.
(9) Thattai, M.; van Oudenaarden, A. Intrinsic noise in gene regulatory networks. *Proc. Natl. Acad. Sci. U. S. A.* **2001**, *98*, 8614−8619.
(10) Huang, C. Y. F.; Ferrell, J. E. Ultrasensitivity in the mitogen-activated protein kinase cascade. *Proc. Natl. Acad. Sci. U. S. A.* **1996**, *93*, 10078−10083.
(11) Elowitz, M. B.; Leibler, S. A synthetic oscillatory network of transcriptional regulators. *Nature* **2000**, *403*, 335−338.
(12) Ideker, T.; Thorsson, V.; Ranish, J. A.; Christmas, R.; Buhler, J.; Eng, J. K.; Bumgarner, R.; Goodlett, D. R.; Aebersold, R.; Hood, L. Integrated genomic and proteomic analyses of a systematically perturbed metabolic network. *Science* **2001**, *292*, 929−934.
(13) Davidson, E. H.; Rast, J. P.; Oliveri, P.; Ransick, A.; Calestani, C.; Yuh, C. H.; Minokawa, T.; Amore, G.; Hinman, V.; Arenas-Mena, C.; et al. A genomic regulatory network for development. *Science* **2002**, *295*, 1669−1678.
(14) Yu, J.; Xiao, J.; Ren, X. J.; Lao, K. Q.; Xie, X. S. Probing gene expression in live cells, one protein molecule at a time. *Science* **2006**, *311*, 1600−1603.
(15) Kar, S.; Baumann, W. T.; Paul, M. R.; Tyson, J. J. Exploring the roles of noise in the eukaryotic cell cycle. *Proc. Natl. Acad. Sci. U. S. A.* **2009**, *106*, 6471−6476.
(16) Van Kampen, N. *Stochastic Processes in Chemistry and Physics*; Elsevier Science B.V.: Amsterdam, 1992.
(17) Wang, J.; Xu, L.; Wang, E. Potential landscape and flux framework of nonequilibrium networks: robustness, dissipation, and coherence of biochemical oscillations. *Proc. Natl. Acad. Sci. U. S. A.* **2008**, *105*, 12271−6.
(18) Feng, H.; Wang, J. Potential and flux decomposition for dynamical systems and non-equilibrium thermodynamics: curvature, gauge field, and generalized fluctuation-dissipation theorem. *J. Chem. Phys.* **2011**, *135*, 234511.
(19) Qian, H. Mesoscopic nonequilibrium thermodynamics of single macromolecules and dynamic entropy-energy compensation. *Phys. Rev. E: Stat. Phys., Plasmas, Fluids, Relat. Interdiscip. Top.* **2001**, *65*, 016102.
(20) Yang, Q.; Ferrell, J. The Cdk1-APC/C cell cycle oscillator circuit functions as a time-delayed, ultrasensitive switch. *Nat. Cell Biol.* **2013**, *15*, 519−525.
(21) Zhao, R.; Deibler, R. W.; Lerou, P. H.; Ballabeni, A.; Heffner, G. C.; Cahan, P.; Unternaehrer, J. J.; Kirschner, M. W.; Daley, G. Q. A nontranscriptional role for Oct4 in the regulation of mitotic entry. *Proc. Natl. Acad. Sci. U. S. A.* **2014**, *111*, 15768−15773.
(22) Li, L.; Wang, J.; Hou, J.; Wu, Z.; Zhuang, Y.; Lu, M.; Zhang, Y.; Zhou, X.; Li, Z.; Xiao, W.; et al. Cdk1 interplays with Oct4 to repress differentiation of embryonic stem cells into trophectoderm. *FEBS Lett.* **2012**, *586*, 4100−7.
(23) Chen, K. C.; Csikasz-Nagy, A.; Gyorffy, B.; Val, J.; Novak, B.; Tyson, J. J. Kinetic analysis of a molecular model of the budding yeast cell cycle. *Mol. Biol. Cell* **2000**, *11*, 369−391.
(24) Tyson, J. J.; Novak, B. Regulation of the eukaryotic cell cycle: Molecular antagonism, hysteresis, and irreversible transitions. *J. Theor. Biol.* **2001**, *210*, 249−263.
(25) Wang, J.; Li, C.; Wang, E. Potential and flux landscapes quantify the stability and robustness of budding yeast cell cycle network. *Proc. Natl. Acad. Sci. U. S. A.* **2010**, *107*, 8195−200.
(26) Li, C.; Wang, J. Landscape and flux reveal a new global view and physical quantification of mammalian cell cycle. *Proc. Natl. Acad. Sci. U. S. A.* **2014**, *111*, 14130−5.
(27) Gerard, C.; Goldbeter, A. Temporal self-organization of the cyclin/Cdk network driving the mammalian cell cycle. *Proc. Natl. Acad. Sci. U. S. A.* **2009**, *106*, 21643−21648.
(28) Gerard, C.; Goldbeter, A. From simple to complex patterns of oscillatory behavior in a model for the mammalian cell cycle containing multiple oscillatory circuits. *Chaos* **2010**, *20*, 045109.
(29) Gerard, C.; Goldbeter, A. Entrainment of the Mammalian Cell Cycle by the Circadian Clock: Modeling Two Coupled Cellular Rhythms. *PLoS Comput. Biol.* **2012**, *8*, e1002516.
(30) Wang, J.; Xu, L.; Wang, E.; Huang, S. The potential landscape of genetic circuits imposes the arrow of time in stem cell differentiation. *Biophys. J.* **2010**, *99*, 29−39.
(31) Wang, J.; Zhang, K.; Xu, L.; Wang, E. Quantifying the Waddington landscape and biological paths for development and differentiation. *Proc. Natl. Acad. Sci. U. S. A.* **2011**, *108*, 8257−62.
(32) Xu, L.; Zhang, K.; Wang, J. Exploring the Mechanisms of Differentiation, Dedifferentiation, Reprogramming and Transdifferentiation. *PLoS One* **2014**, *9*, No. e105216.
(33) Li, C.; Wang, J. Quantifying cell fate decisions for differentiation and reprogramming of a human stem cell network: landscape and biological paths. *PLoS Comput. Biol.* **2013**, *9*, No. e1003165.
(34) Zhang, K.; Wang, J. Exploring the Underlying Mechanisms of the Xenopus laevis Embryonic Cell Cycle. *J. Phys. Chem. B* **2018**, *122*, 5487−5499.
(35) Kim, S. Y.; Ferrell, J. E. Substrate competition as a source of ultrasensitivity in the inactivation of Wee1. *Cell* **2007**, *128*, 1133−1145.
(36) Trunnell, N. B.; Poon, A. C.; Kim, S. Y.; Ferrell, J. E. Ultrasensitivity in the Regulation of Cdc25C by Cdk1. *Mol. Cell* **2011**, *41*, 263−274.
(37) Huang, S.; Guo, Y. P.; May, G.; Enver, T. Bifurcation dynamics in lineage-commitment in bipotent progenitor cells. *Dev. Biol.* **2007**, *305*, 695−713.
(38) Niwa, H.; Toyooka, T.; Shimosato, D.; Strumpf, D.; Takahashi, K.; Yagi, R.; Rossant, J. Interaction between Oct3/4 and Cdx2 determines trophectoderm differentiation. *Cell* **2005**, *123*, 917−929.
(39) Ralston, A.; Rossant, J. Genetic regulation of stem cell origins in the mouse embryo. *Clin. Genet.* **2005**, *68*, 106−112.

DOI: 10.1021/acs.jpcb.9b00509
J. Phys. Chem. B 2019, 123, 3490−3498